J Therm Anal Calorim (2012) 110:907–915
DOI 10.1007/s10973-011-1985-8

Crystallization kinetics, melting behavior, and RAP of novel etheroatom containing naphthyl polyesters

M. Gazzano · M. Soccio · N. Lotti · L. Finelli · A. Munari

Received: 31 May 2011 / Accepted: 11 October 2011 / Published online: 1 November 2011

Abstract The changes in crystalline phase of poly (butylene naphthalate) (PBN), poly(diethylene naphthalate) (PDEN) and poly(thiodiethylene naphthalate) (PTDEN) upon thermal treatments were evaluated by X-ray diffraction technique. The melting behavior and the crystallization kinetics of the polymers under investigation were investigated by means of differential scanning calorimetry. Multiple endotherms were evidenced in PBN and PTDEN, due to melting and recrystallization processes. By applying the Hoffman–Weeks' method, the T_m° of PBN, PDEN, and PTDEN was derived: the introduction of ethero-atoms along PBN polymer chain causes a decrement of T_m° value. The isothermal crystallization kinetics was analyzed according to the Avrami's treatment: the presence of ether-oxygen or sulphur atoms in the chain deeply reduces the PBN ability of crystallizing. Finally, no interphase was evidenced both in PDEN and PTDEN.

Keywords Poly(butylene naphthalate) · Diethylene glycol · Thiodiethylene glycol · X-ray diffraction · Isothermal crystallization

Introduction

In order to improve the heat resistance of phenyl polyesters, some naphthyl polyesters have been developing, such as poly(ethylene 2,6-naphthalate) (PEN) and poly(butylene 2,6-naphthalate) (PBN). In particular, PBN is characterized by excellent mechanical, thermal, gas barrier, and electrical properties, which permit its use as biaxially oriented films, fibers, connectors, switches, coil bobbins, ignition coils fuel sensors, fuel tanks, and hoses. PBN is a linear aromatic polyester whose chemical structure is characterized by flexible butylene groups and stiff naphthalate rings, which can undergo strong interchain interactions. It is semicrystalline with a glass transition temperature (T_g) of about 323–355 K (the wide range of values is due to the difficulty of obtaining samples in a completely amorphous state) and a melting temperature of about 513 K [1–5]. It has been reported that PBN possesses two crystalline structures (α and β) and that the transition between these two phases can take place reversibly by mechanical deformation [6]. Ju et al. investigated the crystalline forms of PBN samples obtained by different thermal treatments in bulk: the α form develops by annealing a quenched sample in the solid state or by crystallizing PBN from the static melt at temperatures lower than 498 K. On the other hand, an exclusive β' form is generated by performing non-isothermal crystallization from the melt at extremely low cooling rate (0.1 K min^{-1}). This thermally prepared β' form is characterized by WAXD profile similar to that of the β form obtained by highly mechanical deformation, except for the substantial d-spacing deviation in (0-11) and (010) planes [7]. Nevertheless, if PBN is melt crystallized at high T_c, both α and β' forms are obtained simultaneously, and their relative ratio is dependent on the adopted crystallization temperature.

Recently, poly(butylene naphthalate) (PBN), poly(thiodiethylene naphthalate) (PTDEN), and poly(diethylene naphthalate) (PDEN) samples were synthesized in our laboratories and characterized in terms of molecular,

M. Gazzano
Istituto per la Sintesi Organica e la Fotoreattività, CNR,
Via Selmi 2, 40126 Bologna, Italy

M. Soccio · N. Lotti (✉) · L. Finelli · A. Munari
Dipartimento di Ingegneria Civile, Ambientale e dei Materiali,
Università di Bologna,
Via Terracini 28, 40131 Bologna, Italy
e-mail: nadia.lotti@mail.ing.unibo.it

thermal, and mechanical properties, to analyze the effect of the presence of sulphur or ether-oxygen atoms along the PBN chains [5].

It is well known that the morphological structure (size, shape, and perfection orientation of crystallites), which is formed by crystallization from the molten state influences strongly the properties of a polymeric material. Therefore, the behavior of polymers during isothermal crystallization from the melt has a relevant technological importance to optimize process conditions and control the properties of the final products. Moreover, it has to be emphasized that in recent years, the study of the rigid-amorphous phase present in some polymers has aroused a growing interest. In general, the structure of most semicrystalline polymers cannot be simply described by means of a two-phase model, consisting of crystalline and amorphous phases. As a consequence, a third phase, the so called "rigid-amorphous phase" (RAP) or "inter-phase" between crystalline and amorphous layers has to be taken into consideration in these structures. In this view, herein the melting behavior and the isothermal crystallization kinetics of PTDEN and PDEN were investigated and the results compared with those concerning homopolymer PBN. Finally, differential scanning calorimetry (DSC) as well as X-ray diffraction (XRD) measurements were used to determine the possible existence of a rigid-amorphous fraction both in PTDEN and PDEN.

Experimental

Materials

PBN, PTDEN, and PDEN were synthesized according to the well-known two-stage polycondensation procedure, as previously reported [5], starting from 2,6-dimethylnaphthalate (DMN) and the appropriate glycol (1,4-butanediol (BD), diethylene glycol (DEG), and thiodiethylene glycol (SDEG)), according to the kind of polyesters to be prepared, with titanium tetrabutoxide ($Ti(OBu)_4$) as catalyst. The monomeric units can be represented as follows:

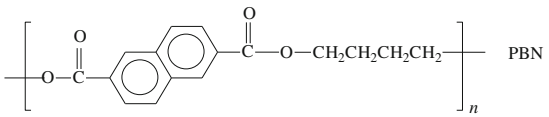

PBN

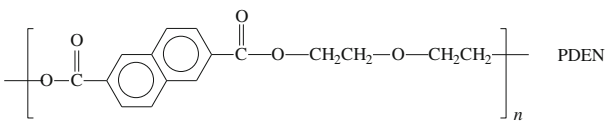

PDEN

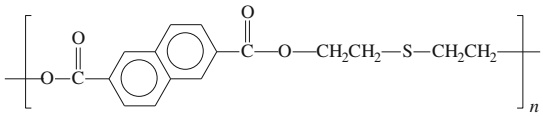

PTDEN

The polymers were previously characterized by some of us from the molecular and thermal point of view [5]. The chemical structure was confirmed by means of ^{1}H-NMR, and the number average molecular mass was determined by GPC. The molecular and thermal characterization data are reported in Table 1.

Calorimetric measurements

The isothermal crystallization behavior of PBN, PDEN, and PTDEN was investigated with a Perkin-Elmer DSC7 calorimeter. The external block temperature control was set at 213 K. All the measurements were carried out under a nitrogen atmosphere to minimize the oxidative degradation. The instrument was calibrated with high-purity standards (indium and cyclohexane) for melting temperature and heat of fusion. Heating rates of 5, 10, 20, and 40 K min^{-1} were used whenever needed. Relatively small size samples (ca. 5 mg) were used to minimize the effect of the thermal conductivity of the polymer; a fresh specimen was used for each run.

To erase the previous thermal history, the samples were heated to about 40 K above fusion temperature at a rate of 20 K min^{-1}, held there for 3 min, and then rapidly cooled by liquid nitrogen to the predetermined crystallization temperature T_c. The T_c range was chosen to avoid crystallization on the cooling step and to obtain crystallization times no longer than 60 min. The heat flow evolving during the isothermal crystallization was recorded as a function of time, and the completion of the crystallization process was detected by the leveling of the DSC trace. For a better definition of the starting time (t_{start}), for each isothermal scan a blank run was also performed with the same sample at a temperature above the maximum of melting endotherm at which no phase change occurred [8]. The blank run was subtracted from the isothermal crystallization scan and the start of the process was taken as the intersection of the extrapolated baseline and the resulting exothermal curve. The isothermally crystallized samples were then heated directly from T_c up to melting at 10 K min^{-1}. The melting temperature (T_m) was taken as the peak value of the endothermic phenomenon of the DSC curve.

The melting enthalpy of samples with different crystallinity degree was measured with the aim of obtaining information about the possible presence of a crystal–amorphous interphase. In order to obtain samples characterized by different crystal/amorphous ratios, the polymers were partially melted in DSC by heating to various

Table 1 Molecular and thermal characterization data

Polymer	M_n^a	M_w/M_n^b	1st scan		2nd scan					
			T_m^c/K	ΔH_m^d/J g^{-1}	T_g^e/K	Δc_p^f/J g^{-1} K^{-1}	T_c^g/K	ΔH_c^h/J g^{-1}	T_m/K	ΔH_m/J g^{-1}
PBN	23,000	2.13	513	57	352	0.104	–	–	513	50
PDEN	35,000	1.98	452	56	331	0.368	–	–	–	–
PTDEN	16,000	2.25	433	40	320	0.343	409	3	433	3

[a] Number average molecular mass

[b] Polydispersity index

[c] Melting temperature

[d] Heat of fusion

[e] Glass transition temperature

[f] Specific heat increment

[g] Crystallization temperature

[h] Heat of crystallization

temperatures in the melting range, quickly cooled inside the instrument below the glass transition temperature and reheated at 20 K min^{-1}.

The specific heat increment Δc_p, associated with the glass transition of the amorphous phase, was calculated from the vertical distance between the two extrapolated baselines at the glass transition temperature. The heat of fusion of the crystal phase developed in spite of the melt quenching was approximately calculated from the difference between the enthalpy associated with the melting endotherm and the cold-crystallization exotherm.

Wide-angle X-Ray scattering measurements

XRD patterns were carried out using a PANalytical X'PertPro diffractometer equipped with a fast solid state X'Celerator detector and a copper target ($\lambda = 0.15418$ nm). Data were acquired in the 5°–60° 2θ interval, by collecting 80 s at each 0.08° step. In situ XRD analysis was also performed using an Anton Paar TTK-450 sample stage. The sample was melted in the stage at 40 K above the melting temperature, kept at this temperature for 3 min, and then cooled at very fast speed to 273 K. Subsequently, the temperature was increased at 20 K min^{-1}, and the data collection was performed at fixed temperatures by scanning from 6 to 40° 2θ degrees counting 20 s each 0.1° step (the features of the X'Celerator detector each scan was completed in 40 s). The indexes of crystallinity (χ_c) were evaluated from the X-ray powder diffraction profiles by the ratio between the crystalline diffraction area (A_c) and the total area of the diffraction profile (A_t), $\chi_c = A_c/A_t$. The crystalline diffraction area has been obtained from the total area of the diffraction profile by subtracting the amorphous halo. The incoherent scattering was taken in the due consideration.

Results and discussion

Preliminarily, the nature of crystalline phase present in the three homopolymers under investigation has been evaluated. The XRD patterns of the as-prepared PBN, PDEN, and PTDEN are shown in Fig. 1, as it can be seen, in all cases the reflections are large, revealing the small dimensions of ordered domains and moreover some of them are the result of several convoluted peaks. Nevertheless, the shape of the profiles are characteristic of each polymer; in particular, PBN shows the diffraction peaks characteristic of the α-form [6]. Since at present the crystalline structures of PDEN and PTDEN have been not yet described in the

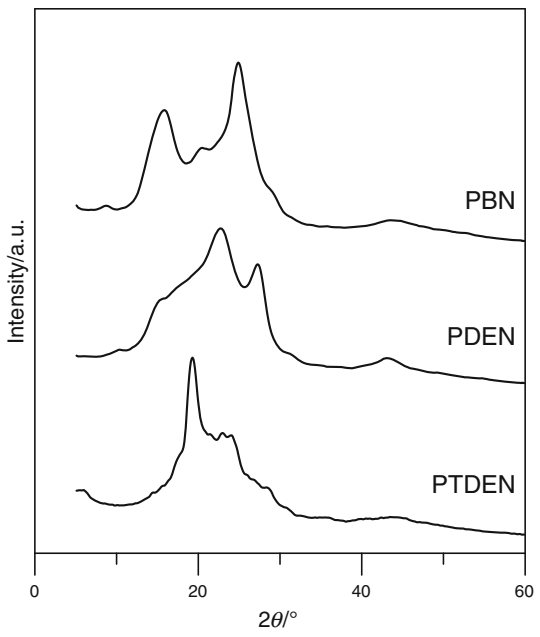

Fig. 1 X-ray diffraction patterns of the "as prepared" samples

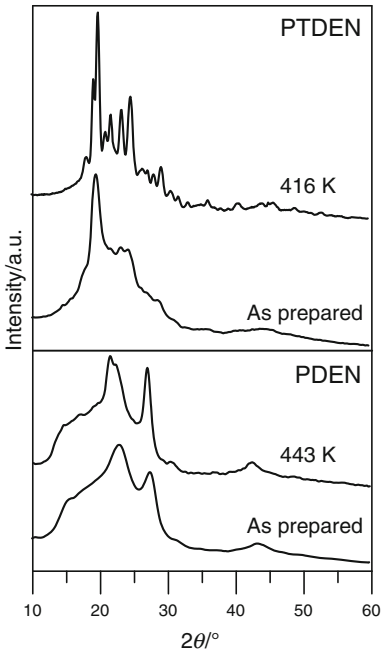

Fig. 2 XRD patterns of the "as prepared" and well-crystallized samples for PTDEN and PDEN

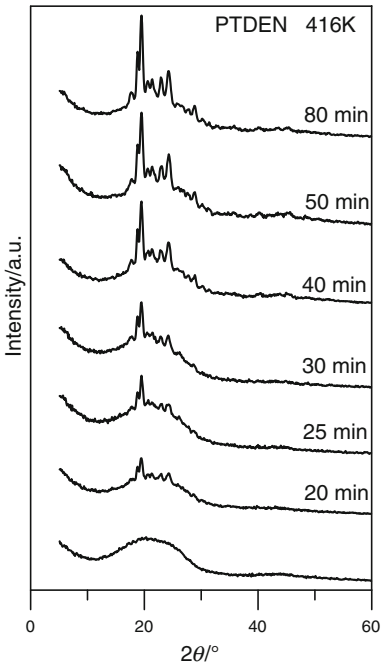

Fig. 3 XRD patterns of PTDEN collected during the isothermal crystallization at 416 K

literature, and several trials were carried out to increase their pattern quality.

The better patterns obtained are reported in Fig. 2.

The best pattern for PTDEN was obtained by melt isothermal crystallization at 416 K. The reflections became very sharp and resolved and were found at the 2θ angles 6.2°, 17.9°, 18.9°, 20.7°, 21.5°, 23.1°, 24.4°, 26.9°, 27.8°, and 28.9°. Annealing for 24 h at 443 K of PDEN caused only a modest increase in crystallinity and peak resolution. The corresponding pattern shows the main reflections at 9.6°, 21.5°, 22.3°, 26.9°, 30.3°, and 42.4°, and two others having very weak intensity also at 14.6° and 17.1° and many others at the highest angles. The isothermal crystallization process at 416 K of PTDEN was observed by in situ XRD analysis: the data collected are shown in Fig. 3. After 20 min, some peaks rose from the amorphous halo. Their intensity increased with time up to get the maximum value 80 min after the starting of the process.

As far as PDEN homopolymer is concerned, samples isothermally crystallized from the melt at different temperature have been investigated: the corresponding WAXS patterns are reported in Fig. 4.

As can be seen in Fig. 4 and from the data shown in the inset, the crystallinity increased from 17 to 26%, even though there was only a modest improvement of the pattern quality and resolution respect to the "as prepared" sample.

Finally, the behavior of the parent homopolymer PBN was also investigated to confirm the results reported in the literature [7]. In Fig. 5, the XRD patterns of PBN samples

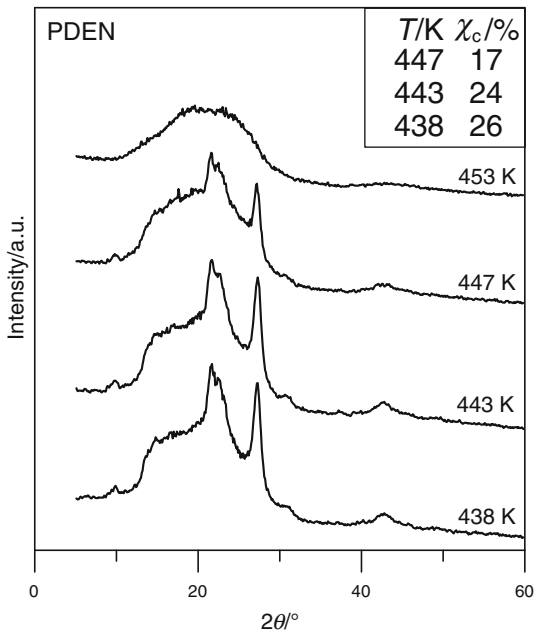

Fig. 4 XRD patterns of PDEN samples isothermally crystallized from the melt at the reported temperatures. In the *inset* the crystallinity index values are reported

isothermally crystallized from the melt at different temperatures are shown: as it can be seen, in all cases, the phase which developed is α phase, but at 498 K two very small reflections, located at angles where β-phase has the most intense reflections, appeared.

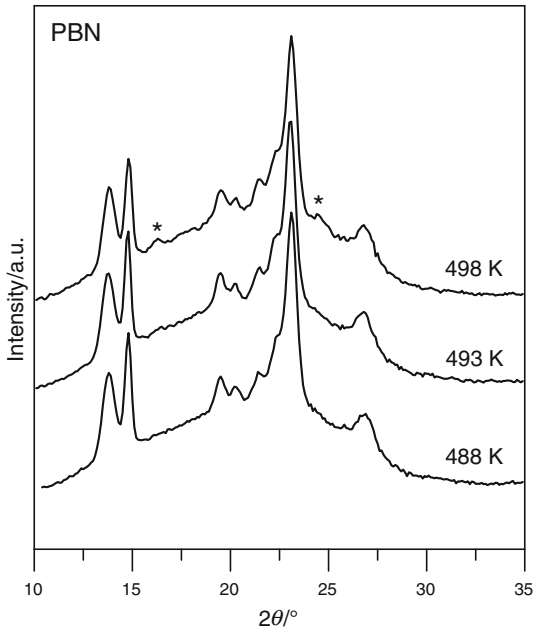

Fig. 5 XRD patterns of PBN samples isothermally crystallized from the melt at the reported temperatures; *asterisks* indicate the position of the two most intense reflections of β-PBN

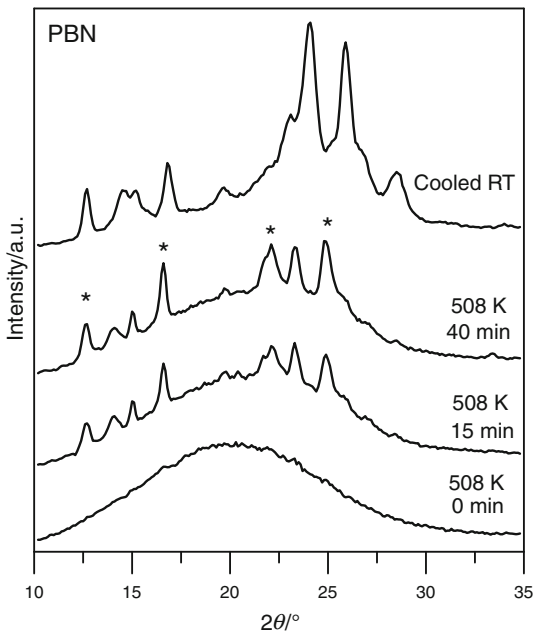

Fig. 6 XRD patterns collected during the isothermal crystallization of PBN at 508 K and after the sample was cooled at room temperature. *Asterisks* indicate the position of the most intense reflections of β-PBN

To verify the coexistence of α and β forms at temperatures higher than 493 K, PBN was isothermally crystallized from the melt at 508 K and XRD patterns were collected during the isothermal crystallization process as shown in Fig. 6, the contemporary crystallization of α- and β-PBN phases occurred. Moreover, the β/α ratio was found to increase with crystallization time, but it reverse going back to room temperature.

Melting behavior

Afterward, the melting behavior of the samples isothermally crystallized from the melt was considered. Figure 7 shows some typical calorimetric traces of PBN, PDEN, and PTDEN, isothermally crystallized at various temperatures (T_c) according to the thermal treatment described in the "Experimental" section.

In the case of PBN, all the DSC curves are characterized by multiple endotherms, which have been labeled as I, II, *, and III, respectively. Melting peak I is present at all the T_c's investigated and appears as a small peak at a temperature which is about 5 K higher than T_c. Melting peak II is also always present: its position shifts to higher temperature and its magnitude increases with increasing T_c. With respect to melting peaks * and III, they appear at all the T_c's investigated and their position remains unchanged with T_c. As clearly shown in Fig. 7, the ratio of the area of melting peak * to that of melting peak III decreases as T_c is increased. Multiple endotherms appear also in the thermograms on heating of PTDEN, whose peaks have been labeled with roman numerals from I to III in order of increasing temperature. In this case too, a dependence of the position and intensity of the endotherms on temperature can be observed: in particular, endotherm I temperature is approximately 5 K above T_c; the position of melting peak II shifts to higher temperature and its magnitude increases with increasing the crystallization temperature. As regards endotherm III, its position remains unchanged, whereas the magnitude decreases with increasing T_c. Both for PBN and PTDEN, the observed dependence of the multiple endotherms on the crystallization temperature permits to hypothesize the origin of each peak. In particular, peak I can be considered the typical "annealing peak" and can be associated with the melting of poorer crystals that grow at T_c between the larger crystals. Endotherm II can be ascribed to the fusion of crystals grown by normal primary crystallization during the isothermal period at T_c; its dependence on the crystallization temperature, in terms of both peak position and area, suggests that thicker crystalline lamellae develop with increasing T_c. The high temperature melting peak (* and III in the case of PBN and III for PTDEN) can be explained as the result of the melting of crystals of higher stability and perfection, grown during the heating run as a consequence of recrystallization or reorganization of crystals initially formed during isothermal crystallization. Finally, in the case of PDEN, only the "annealing peak" and the endotherm due to the fusion of normal primary crystals are observed. In general, there are

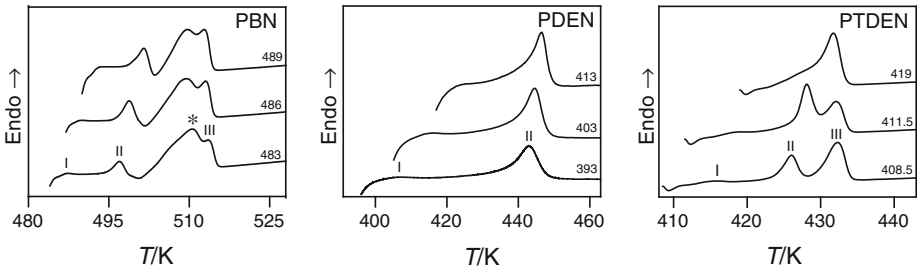

Fig. 7 DSC melting endotherms after isothermal crystallization at the indicated T_c's (heating rate: 10 K min^{-1})

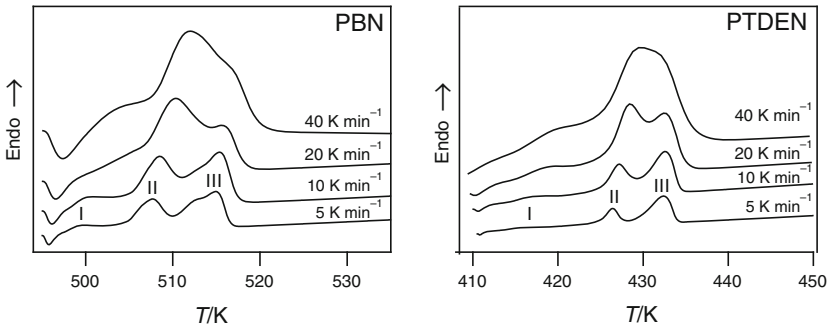

Fig. 8 DSC melting endotherms of PBN and PTDEN scanned at the indicated heating rates after isothermal crystallization at 495 and 410 K, respectively. The curves have not been corrected for changes in the instrumental signal with heating rate

two main reasons for the appearance of multiple melting endotherms. More than one DSC endothermic peak can result from the melting of different crystal types within the samples, each present before thermal treatment [9–11]. Multiple endothermic peaks can also be due to partial melting of some or all of the original material and its reorganization into higher ordered material during the thermal analysis before finally melting [12, 13]. In order to confirm the possibility of melting-recrystallization processes in the samples under investigation, the effect of the heating rate on the melting phenomenon was evaluated. As shown in Fig. 8, the magnitude of melting peak due to the primary crystal increases as the heating rate is increased, contrarily to the highest temperature melting peak, the intensity of which regularly decreases with the heating rate.

The higher value of the heat of fusion of the melting peak of the primary crystal at the faster heating rate indicates that the crystals formed at T_c do not have enough time to melt and recrystallize, confirming therefore a mechanism based on melting and recrystallization of less perfect crystallites into thicker crystals melting at higher temperature.

In addition, it is worth remembering that the multiple melting endotherm phenomenon observed in PBN has been already subject of intense studies and has been ascribed to melting/recrystallization processes taking place during the DSC scan [14–17]. In the case of PTDEN too, it is plausible to ascribe the multiple melting peaks to melt-recrystallization processes occurring during the DSC scan.

In order to compare the crystallization rates of the samples under investigation, it is of great importance the measurement of the equilibrium melting temperature (T_m°) to establish the rate of crystallization dependence on the degree of undercooling, $\Delta T = T_m^\circ - T_c$. One of the most commonly used procedures to determine T_m° is the Hoffman–Weeks method [18]. The popularity of this approach is due to its simplicity, needing only the experimental melting temperature of the crystallites formed at T_c. Nevertheless, recently, Marand and co-workers [19, 20] discussed the validity of the assumption that represents the basic premise of the linear Hoffman–Weeks treatment, i.e., the thickening coefficient for lamellae, γ, taken as independent of T_c and time. As demonstrated by some results that appeared in the literature [19–24], the linear extrapolation, when carried out for lamellar crystals exhibiting a constant γ value, invariably underestimates T_m° and leads to an overestimation of the γ value. In fact, the Hoffman–Weeks procedure does not account for a significant contribution to the difference between melting and crystallization temperatures arising from both the temperature dependence of the fold surface free energy and the thickness increment above the minimum (thermodynamic) lamellar thickness. Neglecting this contribution causes an underestimation of the equilibrium melting temperature and an overestimation of the thickening coefficient. Notwithstanding the above limitations, the experimental melting temperatures (T_m) of PBN, PDEN, and PTDEN crystallized at different T_cs were used to obtain information on the equilibrium melting temperature (T_m°) by means of the Hoffman–Weeks' relationship [18]:

$$T_m = T_m^\circ(1 - 1/\gamma) + T_c/\gamma \quad (1)$$

where γ is a factor which depends on the lamellar thickness. More precisely $\gamma = l/l^*$ where l and l^* are the

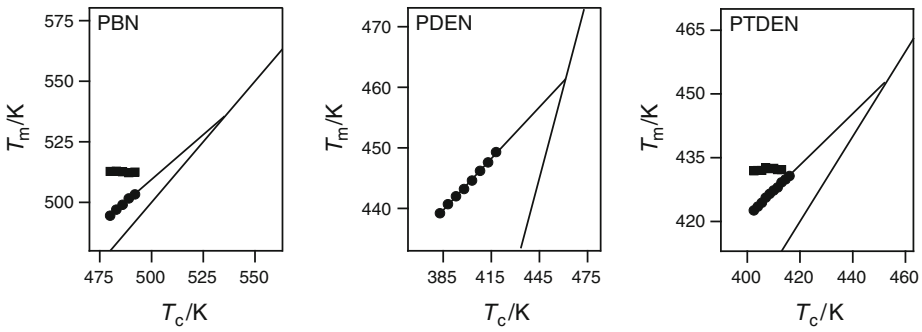

Fig. 9 Peak temperatures of (*filled circle*) II and (*filled square*) III endotherms as a function of T_c and linear extrapolation according to the Hoffman–Weeks treatment

thickness of the grown crystallite and of the critical crystalline nucleus, respectively. Note that Eq. 1 correctly represents experimental data only when γ is constant and the slope of the curve in a plot of T_m versus T_c is approximately equal to 0.5.

The peak values of endotherm II and III as a function of T_c are plotted in Fig. 9 for all the polymers under investigation.

Endotherm II is clearly related to the original main crystal population, and its location reflects the higher perfection of the crystals grown at higher temperatures. Melting endotherm III is observed at a rather constant temperature characteristic of the material partially recrystallized into a more stable form on heating. As a matter of fact, with the increment of T_c, the originally grown crystals improve their degree of perfection up to a point at which no further recrystallization can occur during the DSC run, and endotherm III disappears (see the case of PTDEN). In Fig. 9, the linear extrapolation of experimental data up to the $T_m = T_c$ line is also drawn, and the T_m° values obtained are 534, 463, and 450 K, for PBN, PDEN, and PTDEN, respectively. As far as PBN homopolymer is concerned, T_m° turned out to be lower than those reported by other Authors and this is probably due to the much lower molecular mass of the sample under investigation [14, 15]. Moreover, the melting point is found to be affected by the chemical structure of the polymers and changes as follows: $T_m^\circ{}_{PBN} > T_m^\circ{}_{PDEN} > T_m^\circ{}_{PTDEN}$. In order to explain such trend, it has to be reminded that the melting temperature value of a polymer depends on several factors, among which chain flexibility and intermolecular bonding. The lower melting temperatures for PDEN and PTDEN with respect to PBN can be explained as due to the higher flexibility induced in the polymer chain by the presence of ether-oxygen or sulphur atoms. Finally, PDEN melts at higher temperature in respect to PTDEN. This behavior can be explained as due to the higher polarity of oxygen atoms in respect to sulphur ones, which implies stronger interchain interactions as well as to the kind of crystalline structure and chain packing.

Isothermal crystallization kinetics

The crystallization kinetics of PDEN and PTDEN unfortunately could not be investigated because no appreciable crystallization of the samples occurs in reasonable time. The impossibility to investigate the melt isothermal crystallization kinetics of PDEN and PTDEN indicates that the introduction of ethero-atoms along PBN polymer chain decreases significantly the ability of crystallizing, probably due to high difficulties of stabilization of the required long-range alignment.

As concerns PBN, the crystallization temperature range where only α-phase forms were considered.

As well known, the analysis of the isothermal crystallization kinetics can be carried out on the basis of the Avrami equation [25]:

$$X_t = 1 - \exp[-k_n(t - t_{start})^n] \quad (2)$$

where X_t is the fraction of polymer crystallized at time t, k_n the overall kinetic constant, t is the time of the isothermal step measured from the achievement of the temperature control, t_{start} the initial time of the crystallization process, as described in the experimental section, and n the Avrami exponent, which is correlated with the nucleation mechanism and the morphology of the growing crystallites. X_t can be calculated as the ratio between the area of the exothermic peak at time t and the total measured area of crystallization. The value of the kinetic constant k_n is also frequently obtained by means of the following relationship:

$$k_n = \ln 2 / t_{1/2}^n \quad (3)$$

where $t_{1/2}$ is the crystallization half-time, defined as the time required to reach $X_t = 0.5$.

It is likewise worth remembering that Eq. 2 is usually applied to the experimental data in the linearized form, by plotting $[\ln(-\ln(1 - X_t)]$ as a function of $\ln(t - t_{start})$, permitting the determination of n and k_n from the slope and the intercept, respectively.

The crystallization half-time $t_{1/2}$, the parameter n, and the kinetic constants k_n are collected in Table 2, as can be seen, for all the samples under investigation, the overall

Table 2 Kinetic parameters for the isothermal crystallization of α-PBN

T_c/K	$t_{1/2}$/min	n	k_n/s^{-n}
480	0.6	2.80	5.4×10^{-5}
483	0.8	2.90	$1{,}1 \times 10^{-5}$
486	1.6	2.90	3.9×10^{-6}
489	2.5	3.10	2.7×10^{-7}
492	4.1	2.90	1.1×10^{-7}
495	6.4	2.80	8.5×10^{-8}
498	11.0	2.9	4.3×10^{-8}

kinetic constant k_n regularly decreases with increasing T_c, as usual at low undercooling, where the crystal formation is controlled by nucleation.

The Avrami exponent n is close to 3 for all the crystallization temperatures investigated, indicating that the crystallization process originates from predetermined nuclei and is characterized by three-dimensional spherulitic growth.

Rigid-amorphous phase

As is well known, most of the highly ordered and rigid semicrystalline polymers are characterized by the presence of the so called "rigid-amorphous phase", such as in the case of poly(ethylene terephthalate) [26], poly(butylene terephthalate) [27], and poly(propylene terephthalate) [28], to cite only the poly(alkylene phthalate)s. To the best of our knowledge, nothing is reported in the literature on PBN, PDEN, and PTDEN. Unfortunately, only the ethero-atom containing polyesters could be investigated, being not able to obtain samples of PBN characterized by different crystal/amorphous ratio because of its very high crystallization rate.

To evaluate the existence of a rigid-amorphous phase in the polyesters under investigation, we examined the relationship between Δc_p at T_g and ΔH_m of samples with different crystal/amorphous ratios. The experimental ΔH_m versus Δc_p data of PDEN and PTDEN, plotted in Fig. 10, show a very good linear fit: as expected, Δc_p steadily decreases as the melting enthalpy (proportional to the degree of crystallinity) increases. The extrapolation to $\Delta c_p = 0$ gives a value of 78 and 57 J g^{-1} for ΔH_m° of PTDEN and PDEN, respectively. A different method was also used for the calculation of ΔH_m°. The enthalpies of fusion of samples with different amorphous/crystal ratio, determined by DSC measurements, were plotted as a function of the corresponding crystallinity degree estimated by means of X-ray analysis (see Fig. 10 right panels).

The melting enthalpy regularly increases as the crystallinity increases, and the experimental data are well

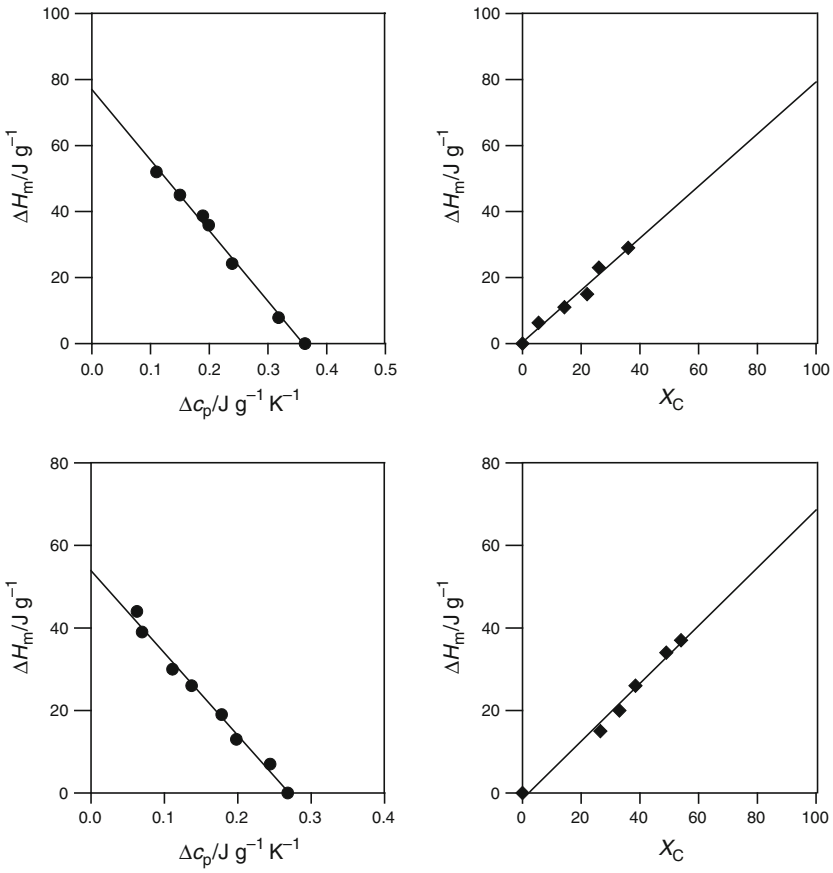

Fig. 10 ΔH_m as a function of (*left panel*) Δc_p at T_g and (*right panel*) X-ray crystallinity for: *upper plots* PTDEN, *lower plots* PDEN

represented by a straight line. ΔH_m of the perfect crystal was obtained by extrapolation to a crystallinity of 100%. The values of ΔH_m° were 80 and 65 J g^{-1} for PTDEN and PDEN, respectively, in good agreement with those obtained from the $\Delta H_m - \Delta c_p$ plots of Fig. 10 (left panels), proving that neither for PTDEN nor for PDEN rigid-amorphous phase has to be postulated. This result could be related to the higher polymer chain flexibility in PTDEN and PDEN (T_{gPDEN} and T_{gPTDEN} lower than T_{gPBN}).

Conclusions

The data obtained display that the introduction along PBN polymer chain of ether-oxygen or sulphur atoms lead to significant variations in the final properties. In particular,

- the melting point decreases, due to the higher flexibility of polymer chain and to a lower chain symmetry;
- the ability to crystallize is deeply lowered, due to a too flexible chain in ether atoms-containing polyesters which allow extensive convolution thereby preventing stabilization of the required long-range alignment.

Finally, the increased chain flexibility in PDEN and PTDEN could explain the absence of rigid-amorphous phase in these two polymers.

References

1. Lee SC, Yoon KH, Kim JH. Crystallization kinetics of poly(butylene 2,6-naphthalate) and its copolyesters. Polym J. 1997;29:1–6.
2. Yamanobe T, Matsuba H, Imai K, Hirata A, Mori S, Komoto T. Structure and physical properties of naphthalene containing polyesters. I. Structure of poly(butylene 2,6-naphthalate) and poly(ethylene 2,6-naphthalate) as studied by solid state NMR spectroscopy. Polym J. 1996;28:177–81.
3. Jakeways R, Ward IM, Wilding MA, Hall IH, Desborough IJ, Pass MG. Crystal deformation in aromatic polyesters. J Polym Sci Polym Phys Ed. 1975;13:799–813.
4. Papageorgiou G, Karayannidis G. Observations during crystallization of poly(ethylene-co-butylene naphthalene-2,6-dicarboxylate). Polymer. 2001;42:8197–205.
5. Soccio M, Finelli L, Lotti N, Siracusa V, Ezquerra TA, Munari A. Novel ethero atoms containing polyesters based on 2,6-naphthalendicarboxylic acid: a comparative study with poly(butylene naphthalate). J Polym Sci. 2007;45:1694–703.
6. Watanabe H. Stretching and structure of poly(tetramethylene 2,6-naphthalenedicarboxylate) films. Kobunshi Ronbunshu. 1976;33:229–37.
7. Ju MY, Huang JM, Chang FC. Crystal polymorphism of poly(butylene-2,6-naphthalate) prepared by thermal treatments. Polymer. 2002;43:2065–74.
8. Marand H, Alizadeh A, Farmer R, Desai R, Velikov V. Influence of structural and topological constraints on the crystallization and melting behavior of polymers. 2. poly(arylene ether ether ketone). Macromolecules. 2000;33(9):3392–403.
9. Chung JS, Cebe P. Melting behavior of poly(phenylene sulfide). 2. multiple-stage melt crystallization. Polymer. 1992;33(11):2312–24.
10. Lemstra PJ, Schouten AJ, Challa G. Secondary crystallization of isotatic polystyrene. J Polym Sci Polym Phys Ed. 1974;12(8):1565–74.
11. Minakov AA, Mordvinsted DA, Schick C. Melting and reorganization of poly(ethylene terephthalate) on fast heating (1000 K/s). Polymer. 2004;45(11):3755–63.
12. Kong Y, Hay JN. Multiple melting behaviour of poly(ethylene terephthalate). Polymer. 2002;44(2):623–33.
13. Papageorgiou G, Karayannidis G. Multiple melting behaviour of poly(ethylene-co-butylene naphthalate-2,6-dicarboxylate)s. Polymer. 1999;40:5325–32.
14. Ju M, Chang FC. Multiple melting behavior of poly(butylene-2,6-naphthalate). Polymer. 2001;42:5037–45.
15. Yasuniwa M, Tsubakihara S, Fujioka T. X-ray and DSC studies on the melt-recrystallization process of poly(butylenes naphthalate). Thermochim Acta. 2003;396:75–8.
16. Yasuniwa M, Tsubakihara S, Fujioka T, Dan Y. X-ray studies of multiple melting behavior of poly(butylene naphthalate). Polymer. 2005;46:8306–12.
17. Hoffman JD, Weeks JJ. Melting process and equilibrium melting temperature of poly(chlorotrifluoroethylene). J Res Natl Bur Stand. 1962;66A(1):13–28.
18. Marand H, Xu J, Srinivas S. Determination of the equilibrium melting temperature of polymer crystals: linear and nonlinear Hoffman–Weeks extrapolations. Macromolecules. 1998;31(23):8219–29.
19. Xu J, Srinivas S, Marand H, Agarwal P. Equilibrium melting temperature and undercooling dependence of the spherulitic growth rate of isotactic polypropylene. Macromolecules. 1998;31(23):8230–42.
20. Wu PL, Woo EM. Linear versus nonlinear determinations of equilibrium melting temperatures of poly(trimethylene terephthalate) and miscible blend with poly(ether imide) exhibiting multiple melting peaks. J Polym Sci. 2002;40(15):1571–81.
21. Al-Hussein M, Strobl G. The melting line, the crystallization line, and the equilibrium melting temperature of isotactic polystyrene. Macromolecules. 2002;35(5):1672–6.
22. Finelli L, Lotti N, Munari A, Gazzano M, Malta V. Poly(thiodiethylene adipate): melting behavior, crystallization kinetics, morphology, and crystal structure. J Polym Sci. 2004;42(3):553–66.
23. Fichera AM, Finelli L, Gazzano M, Lotti N, Munari A. Multiple melting behaviour of poly(thiodiethylene terephthalate): further investigations by means of X-ray and thermal techniques. Macromol Chem Phys. 2004;205(1):63–72.
24. Avrami M. Granulation, phase change and microstructure. Kinetics of phase change III. J Chem Phys. 1941;9:177–84.
25. Schick C, Wigger J, Mischok W. The influence of structural changes on the glass transition in partially crystalline poly(ethylene terephthalate). 3. Glass transition in the interlamellar regions. Acta Polim. 1990;41:137–42.
26. Cheng SZD, Pan R, Wunderlich B. Thermal analysis of poly(butylene terephthalate) for heat capacity, rigid-amorphous content, and transition behavior. Makromol Chem. 1988;189:2443–58.
27. Sisti L, Finelli L, Lotti N, Berti C, Munari A. Memory effect in melting behavior, crystallization kinetics and morphology of poly(propylene terephthalate). e-Polymers. 2003; n° 054, 1–19.
28. Righetti MC, Munari A. Influence of branching on melting behavior and isothermal crystallization of poly(butylene terephthalate). Macromol Chem Phys. 1997;198:363–78.